

# **Influence of Water Vapour on the Zircaloy-4 Oxidation at 700 °C – Stress Determination by In Situ X-Ray Diffraction**

Raphaël ROLLAND<sup>a</sup>, Henri BUSCAIL<sup>a</sup>, Christophe ISSARTEL<sup>a</sup>

<sup>a</sup>*Université de Clermont Auvergne, LVEEM, Laboratoire Vellave sur l'Elaboration et l'Etude des Matériaux, 8 rue J.B. Fabre, CS 10219, 43009 Le Puy-en-Velay, France.*

*[raphael.rolland@udamail.fr](mailto:raphael.rolland@udamail.fr); [henri.buscail@udamail.fr](mailto:henri.buscail@udamail.fr); [christophe.issartel@udamail.fr](mailto:christophe.issartel@udamail.fr)*

**Abstract.** Zircaloy-4 has been oxidised in dry and wet air (15 vol.% H<sub>2</sub>O) at 700 °C. At high temperature and at room temperature X-Ray diffraction shows that the oxide scale is composed of monoclinic zirconia (m-ZrO<sub>2</sub>) and quadratic zirconia q-ZrO<sub>2</sub>. In dry and wet air, growth stress is determined *in situ* at 700 °C on the m-ZrO<sub>2</sub>. In dry air, results show that the compressive growth stress in the oxide oscillates between -1300 ±100 MPa and -600 ±100 MPa. In wet air, compressive growth stress varies from -1000 ±100 MPa to -400 ±100 MPa during the 20 first hour oxidation. Then, the stress level remains constant (-400 ±100 MPa). In dry air stress oscillations can be explained by successive growth stress increases in the growing scale and stress relaxation by perpendicular cracks propagation. The growth stress relaxation process in wet air is related to a higher zirconia grain size.

**Keywords:** Zircaloy-4, *in situ* stress determination, water vapour, high temperature oxidation

## **INTRODUCTION**

Increased attention has been paid to the vulnerability of the Spent Fuel Pools (SFPs) since the Fukushima accident. This vulnerability is of major concern for nuclear safety because SFPs which are large water-filled structures are generally placed outside the reactor containment building so that the fuel clad is the only barrier against fission product release in case of dewatering. To gain knowledge in the above mentioned areas and in order to better evaluate the safety margins, the French Institut de Radioprotection et de Sûreté Nucléaire (IRSN) in collaboration with partners from French universities has launched the DENOPI project. Most of the kinetic investigations on the Zr-based cladding material oxidation in air at high temperature have used bare cladding samples. As far as spent fuels are concerned, the presence of corrosion oxide scale formed during normal operation in reactor has to be considered. In steam atmosphere a protective effect of the pre-oxide is generally observed. Zirconium alloys oxidation resistance is an important factor affecting their use as fuel cladding material in nuclear plants. It is generally accepted that during zirconium alloys oxidation, a dense and protective oxide layer first forms on the metal, giving rise to a reaction rate decreasing with time following a parabolic law [1, 2]. However, after a certain time, a kinetic acceleration appears, corresponding to the breakaway phenomenon. This is related to the loss of protectiveness of the first formed oxide scale. Breakaway can occur several times, leading to corrosion kinetics showing a cyclic behaviour [1, 2]. Post-transition phenomena are also encountered at temperatures expected in

accidental situations, either in steam [3, 4] or oxygen and air atmospheres [5, 6]. The oxidation resistance of a zircaloy, in usual operation conditions as well as in accidental situations, is controlled by the resistance to breakaway of the zirconia scale. The protectiveness loss is attributed to formation of diffusion shortcuts, for example micro-cracks, which were evidenced both for temperatures relevant to in-service conditions [5] and to accidental situations [6]. The breakaway phenomenon can be explained by mechanical considerations [7], but the transition is a complex phenomenon involving coupled chemical, mechanical, microstructural, crystallographic aspects. It has been mentioned that the transition from a protective to a more porous oxide could be associated to a phase transition from tetragonal (t-ZrO<sub>2</sub>) to monoclinic (m-ZrO<sub>2</sub>), close to the metal/oxide interface [8]. From the literature, it has been experimentally demonstrated by X-ray diffraction (XRD) [9-13], Raman spectroscopy [14–17] or transmission electron microscopy [18, 19] that t-ZrO<sub>2</sub> can be detected at the metal/oxide interface in pre-transition scales while it is hardly detected in the scale during the post-transition regime. Various factors such as a deviation from stoichiometry, nanometric grain size, chemical doping, and compressive stress can explain the stabilization of the t-ZrO<sub>2</sub> for temperatures below its thermodynamic stability domain. A high amount of t-ZrO<sub>2</sub> at the metal/oxide interface is often correlated with the presence of high local compressive stress [10, 12, 14, 15, 17]. It has been confirmed by thermodynamic calculations that compressive stress can stabilize the t-ZrO<sub>2</sub> form of zirconia [20], due to the high Pilling– Bedworth ratio of the Zr/ZrO<sub>2</sub> system. It is generally observed that zirconia scales exhibiting the highest compressive stress and thus a better stability of the t-ZrO<sub>2</sub> compound exhibit a better corrosion resistance [10-12, 18]. Most of the authors consider that the t-ZrO<sub>2</sub> to m-ZrO<sub>2</sub> transformation have a detrimental effect on the corrosion resistance. Nevertheless, El Kadiri and co-workers [16] suggest that this phase transformation has a beneficial effect. It is due to the lattice expansion that accompanies the transformation and it contributes to maintain a compressive stress state in the scale and thus delays the oxide breakdown, which occurs when the stress sign change from compressive to tensile firstly close to the external interface. Whatever is the exact role of the t-ZrO<sub>2</sub> to m-ZrO<sub>2</sub> transformation on the breakaway phenomenon, the local stress field that develops in oxide scales formed on Zr alloys appears to be an important factor for the understanding of their oxidation resistance. This explains why stress development in zirconia scales has been studied in the past. In case of loss of primary coolant accident in a light water reactor, the zirconium alloys fuel cladding would be oxidized in air and steam mixtures at high temperatures. From the recent literature review of Guerain and co-workers [21] it appears that no growth stress determinations have been performed on Zircaloy-4 (Zy-4) in dry air or in air/steam gas mixtures close to operating conditions around 500 °C. The key parameter for the understanding of the water vapour effect on the oxidation mechanism is the determination of the stress level in the zirconia scale and in the Zy-4 substrate at high temperature. In order to determine the structure and microstructure of the oxide layers, X-ray diffraction (XRD) analyses have been performed *in situ* under dry air and wet air environments at 700 °C on Zy-4 flat sheet samples. This temperature has been chosen because in case of loss of coolant accident the temperature is rising from the operating temperature up to higher temperatures. Then it is interesting to determine the oxidation mechanism at 700°C which is not necessary the same as the one observed at higher temperatures. The experimental reason is related to the necessary time needed to collect data permitting stress determinations during quite quick oxidation phenomena. The aim of the present work is to show the influence of water vapour on the growth stress developed at high temperature in the oxide scale. The stress evolution during cooling to room temperature will also be determined in order to collect data on the influence of water vapour on the stress relaxation mechanism.

## EXPERIMENTAL PROCEDURES

The material used in the present work is a low tin Zircaloy-4 (Zy-4) alloy. The alloy composition is given in *Table 1*. The specimens, were cut by electro-erosion from a SRA (stress relieved annealed at 480 °C) flat sheet.

**TABLE 1:** Composition of the Zircaloy-4.

<i>Alloy</i>	<i>Composition (wt%)</i>					<i>ppm</i>	<i>ppm</i>	<i>ppm</i>
	<b>Zr</b>	<b>Sn</b>	<b>Fe</b>	<b>Cr</b>	<b>O</b>	<b>C</b>	<b>Nb</b>	<b>H</b>
<b>Zy-4</b>	Balance	1.32	0.21	0.11	0.12	125	< 40	< 3

Flat specimens are 0.43 mm thick and show a total surface area of about 2.6 cm<sup>2</sup>. The *in situ* characterization of the oxide scales was carried out in a MRi high temperature chamber adapted on an Xpert'3 PANalytical  $\Theta$ - $\Theta$  Bragg-Brentano diffractometer (cobalt radiation,  $\lambda k_{\alpha} = 0.179$  nm). The diffraction patterns are registered for two days (48 h) at 700 °C and step by step at 600, 500, 400, 300, 200, 100 and 20 °C during cooling to room temperature. Each stress determination on the alloy or on the oxide scale takes about 2 hours. Concerning stress determination in the alloy, it is only possible for the two first hours, because at 700 °C the oxide scale thickness is rapidly too large and X-ray beam does not cross this layer to analyse alloy. The water vapour experiments were performed in air containing 15 vol.% H<sub>2</sub>O (or 15000 Pa partial pressure). The laboratory compressed flowing air (8 L/h flow rate) is saturated through boiling water. Then, the water bath humidifier acting as a cold point is maintained at 55 °C and controls the water vapour ratio by condensation of the excess water vapour. All the connecting tubes are maintained over 65°C in order to avoid any water condensation. A schematic drawing of the rig was provided in a previous paper [22]. Dry air testing was performed in flowing air at atmospheric pressure. Calibration of the sample temperature was performed with the help of a thermocouple welded on a Zy-4 specimen and placed on the heating element in the high temperature chamber. An infrared pyrometer permits the control of the specimen temperature during oxidation.

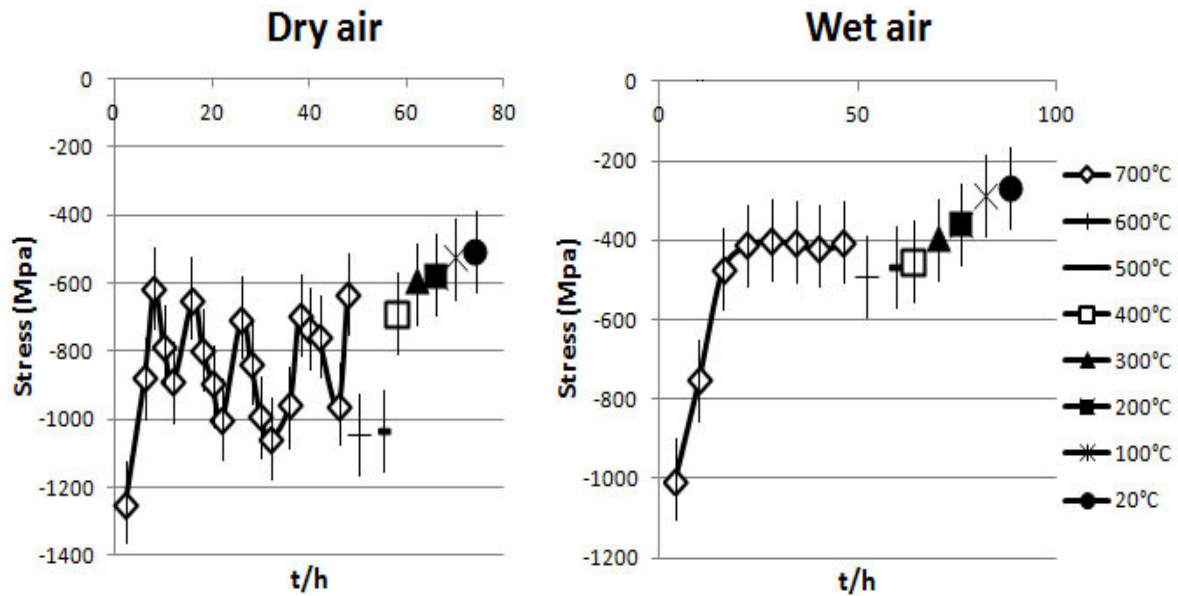
Stress levels in m-ZrO<sub>2</sub> (COD 96-900-7449) were determined by *in situ* X-ray diffraction at 700 °C under atmospheric pressure conditions. Stress determinations were performed by using  $\psi$  goniometer technique, [23, 24] with Co-K<sub>α1</sub> = 0.179 nm radiation, based on the (10-4) planes of the monoclinic m-ZrO<sub>2</sub> structure (84.62° 2 $\Theta$ ). No stress determination is possible on tetragonal zirconia with this technique because the Bragg diffraction angle of the representative peak is too low. The  $\psi$  angle was varied in steps of 2 ° between -38 ° and +38 °. It takes about 2 hours to collect data permitting stress determination. The mean stress  $\sigma_{\phi}$  in the plane of the oxide is obtained from the slope  $(1 + \nu) \cdot \sigma_{\phi} / E$  of the linear relationship between  $\epsilon$  and  $\sin^2 \psi$ , where  $\epsilon$  is the strain, given by  $\Delta d / d$ ,  $d$  being the interplanar spacing. The oxide was assumed to be isotropic with no stress gradients parallel to the surface components. The m-ZrO<sub>2</sub> Young's modulus,  $E$ , was taken as 203 GPa [25] and Poisson's ratio  $\nu$  as 0.32. The technique used is not able to determine the eventual stress gradient inside the oxide scale. Only a mean value is obtained from the whole surface and thickness analysed. Stress determination by XRD only concerns the 10 first  $\mu\text{m}$ . Due to the anionic oxidation process involved during zirconium alloys oxidation, compressive stress are supposed to be mainly generated close to the internal interface. Then, when the oxide scale gets thicker than 10  $\mu\text{m}$ , stress determination should only concern the external part of the oxide scale. Nevertheless, our results obtained in dry air show that the oxide scale structure permits the compressive stress transmission through the scale even though the scale is more than 100  $\mu\text{m}$  thick.

Full Width Half Maximum (FWHM) data were extracted from the fitted peak of the diffraction patterns obtained on m-ZrO<sub>2</sub>. The peak FWHM can be used to determine grain size in the direction normal to the diffracting plane as long as the size is less than about 100 nm although strain within the grain can also cause peak broadening. For this application grains size actually refers to the dimension perpendicular to the sample surface which for columnar grains is the grain column diameter since the diffracting planes measured span the oxide column width rather than the length. In this work the Williamson-Hall analysis [26, 27] of the PANalytical software was used to separate the effects of size and strain broadening on the FWHM. The cross section micrographs are obtained with an optical Leica-Laborlux microscope using x 200 and x 500 magnification.

## RESULTS

*Figure 1* shows the *in situ* growth stress determination in the m-ZrO<sub>2</sub> (COD 96-900-7449) which is the major phase detected during oxidation at 700°C. Stress determination is based on the (10-4) planes of the monoclinic m-ZrO<sub>2</sub> baddeleyite structure. It was performed on Zy-4 specimens in dry and wet air at 700 °C during 48h and successively at 600, 500, 400, 300, 200, 100 and 20 °C during cooling to room temperature. In dry air, results show that the compressive growth stress in the oxide oscillates between -1300 ±100 MPa and -600 ±100 MPa. The oscillation period is about 9 h (approximately 5 oscillations during 48h). The compressive growth stress is relaxed and re-generated, during the scale growth at 700 °C. At 600 °C and at lower temperatures the compressive stress varies from -1100 ±100 MPa to -550 ±100 MPa at room temperature. The progressive stress variation indicates that a relaxation process occurred during cooling.

In wet air compressive growth stress in the m-ZrO<sub>2</sub> scale varies from -1000 ±100 MPa to -400 ±100 MPa during the 20 first hours oxidation. After 20 h oxidation, the compressive growth stress registered remain constant at 700 °C (-400 ±100 MPa). During cooling, the compressive stress varies progressively from -500 ±100 MPa at 600°C to -250 ±100 MPa at room temperature.



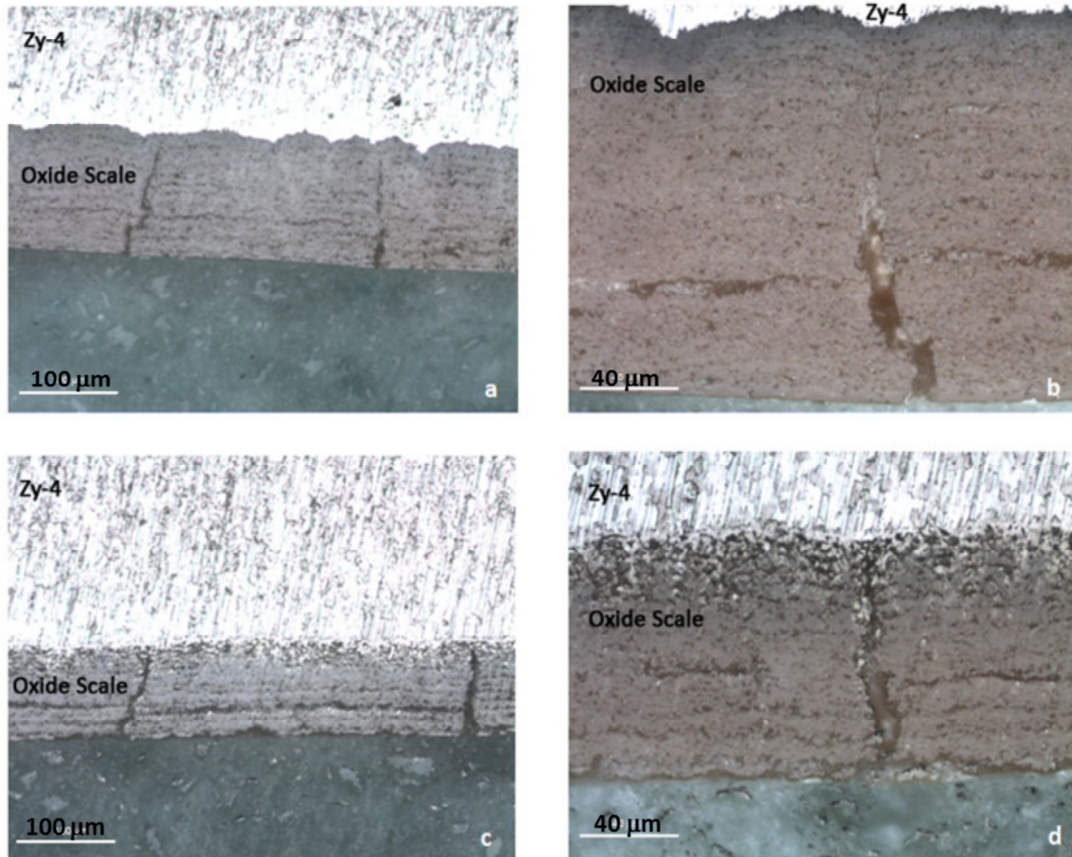
**FIGURE 1.** *In situ* growth stress determined in the m-ZrO<sub>2</sub> scale in dry and wet air at 700 °C and during cooling to room temperature.

Figure 2 shows optical cross sections obtained on Zy-4 specimens after 48 hours oxidation. Figure 2.a) and 2.b) micrographs are obtained after oxidation in dry air with x 200 and x 500 magnifications. Figure 2.c) and d) micrographs are performed after wet air oxidation with x 200 and x 500 magnifications. In dry air, the oxide scale presents longitudinal cracks and perpendicular cracks (perpendicular to the interface). On figure 2.a) approximately 12 longitudinal cracks are observed and two perpendicular cracks are present. It appears on figure 2.b) that the radial cracks do not reach the metal/oxide interface. These cracks are wider at the external interface than at the internal interface indicating an inward propagation of the cracks.

In wet air, micrographs also show longitudinal and perpendicular cracks. The perpendicular crack presented on figure 2.c) and 2.d) reach the metal at the internal interface. The longitudinal cracks have the same morphology in wet and dry air after 48h oxidation at 700 °C. Figure 2 also shows that the oxide scale thicknesses are not similar after oxidation in dry and wet air at 700 °C. The oxide scale is thicker after 48 hours oxidation in dry air (160 µm) than after oxidation in wet air (130 µm).

Before oxidation, X- ray diffraction patterns show the presence of the Zy-4 alloy (COD 96-900-8524). During the first hour oxidation in dry or wet condition, the *in situ* diffraction pattern shows the presence of m-ZrO<sub>2</sub> (COD 96-900-7449), t-ZrO<sub>2</sub> (COD 96-900-9920) and the alloy. After the first hours oxidation it is not possible to detect the alloy anymore. The oxide scale is thicker than the depth penetration of the X-ray beam. After 1 hour oxidation, no new phases are detected on the diffraction patterns until the end of the oxidation test in dry or wet conditions. Only the t-ZrO<sub>2</sub> peak intensity ratio decreases with time because this oxide remains mainly located close to the internal interface. On diffraction patterns obtained during cooling to room temperature, m-ZrO<sub>2</sub> and t-ZrO<sub>2</sub> are still present and no new phases could be detected.

Full Width Half Maximum (FWHM) information was extracted from the fitted peak of the diffraction patterns obtained on m-ZrO<sub>2</sub>. Determination of the zirconia grains size in the oxide scale shows that the size is larger after oxidation in wet air ( $30 \pm 1$  nm in wet air and  $23 \pm 1$  nm in dry air).



**FIGURE 2.** Micrographs obtained on Zy-4 after 48 hours oxidation: a) and b) micrographs obtained after oxidation in dry air x 200 and x 500 magnifications; c) and d) micrographs obtained after oxidation in wet air.

## DISCUSSION

*In situ* growth stress results obtained in dry air show that the compressive growth stress in the oxide oscillates between  $-1300 \pm 100$  MPa and  $-600 \pm 100$  MPa. The oscillation period is about 9h (approximately 5 oscillations in 48h). The compressive growth stress is relaxed and re-grown during oxidation at 700 °C. The stress value determined in our work is comparable to what is observed by some authors ( $-1800 \pm 200$  MPa) at 500 °C on pure Zr and other alloys (M5, Zy-2) [28, 29]. Other authors have also shown that the stress magnitude reaches a maximum value for a scale thickness ranging between 4 and 6 μm on the M5 alloy at 550 °C [30]. In the present work growth stress oscillations at 700 °C in dry air, indicate successions of stress relaxation and stress growth. It is not possible to relate stress oscillations and the number of longitudinal cracks. Our results show approximately 5 growth stress

oscillations within 48 hours and the presence of 12 longitudinal subscales in the lamellar structure. If the stress relaxation is not corresponding to the number of longitudinal cracks, then growth stress relaxation can be attributed to the periodical propagation of perpendicular cracks. In dry air, after the growth of compressive stress up to -1000 MPa, stress relaxation occurred by perpendicular crack propagation near the metal/oxide interface to reach about -600 MPa compressive stress. Then, owing to the anionic oxidation process, growth stress increased again until a maximum value is attained. One should note that the perpendicular cracks formed during dry oxidation do not cross completely the oxide layer. This can explain that the compressive stress is only partially relaxed because the oxide located close to the alloy remains under a compressive state. Figure 1 also exhibits that during cooling to room temperature the compressive stress varies from  $-1100 \pm 100$  MPa down to  $-550 \pm 100$  MPa at room temperature. The progressive stress variation indicates that a relaxation process occurred during cooling due to cracks propagation in the zirconia scale.

In wet air, the *in situ* stress determinations show that compressive growth stress in the m-ZrO<sub>2</sub> scale varies from  $-1000 \pm 100$  MPa to  $-400 \pm 100$  MPa during the 20 first hour oxidation. This implies that the growth stress relaxation also occurred by cracks propagation. After 20 h the compressive growth stress registered remains constant at  $-400 \pm 100$  MPa all along the isothermal part of the test. On figure 1, results also indicate that the compressive growth stress registered in the oxide scale is lower in wet air than in dry air. In wet air, no growth stress oscillations are detected because the oxide scale does not recover a higher compressive stress. During cooling, no important stress relaxation occurred in zirconia scales obtained under wet condition because relaxation has already occurred under isothermal oxidation at 700 °C. In figure 2, cross sections show that perpendicular cracks totally cross the oxide layer after wet air oxidation. It indicates that the mechanical properties of the oxide scale are modified by the water vapour presence in air.

*In situ* growth stress determinations in m-ZrO<sub>2</sub> have shown that the compressive stress is larger in dry air compared to wet air environment at 700 °C ( $-400 \pm 100$  MPa). The lower stress state observed in wet environment is in accordance with the results of Pétigny [10, 11] who has performed a comparative study on the effect of oxygen and steam at 470 °C by using X-ray diffraction. It appears that the average stress magnitudes are larger in dry oxygen than in steam. These results are also consistent with the values obtained by synchrotron X-ray diffraction at 400 °C [31, 32]. As observed in the present work, it has been proposed that under wet atmospheres, the average stress values are very low at the very early oxidation stage and becomes less negative. This behaviour may be related to stress relaxation phenomena taking place early during the formation of the scale [21].

Our results are in accordance with other authors indicating that *in situ* compressive growth stress is higher in dry air compared with wet air at 700 °C. This can be due to an effect of water vapour on the zirconia mechanical properties. Grain size determinations show a higher zirconia grain size after wet air oxidation. The m-ZrO<sub>2</sub> grain size at the external interface is about 23 nm in dry air and 30 nm in wet air. In wet air the grain size is 30% higher. This result is in accordance with the work of Methivier showing that the zirconia grain size is higher when water is present during its synthesis, probably due to a catalytic effect [33]. A higher oxide grain size is also generally related to a weaker oxide state [34, 35]. In the present work, we attribute the growth stress relaxation process in wet air to the higher grain size and a weak oxide scale. In dry air, our results show that zirconia grains are smaller and the oxide layer can accommodate more important compressive stresses before cracking and relaxation. The higher scale plasticity of zirconia in dry air then permits *in situ* stress oscillations. In this case, stress relaxation corresponds to perpendicular crack propagation when oxide layer has attained a critical growth stress, every 9 hours.

Modification of the zirconia grain size by water can be related to a modification of the oxide growth mechanism. Some authors have proposed a transport mechanism of H<sub>2</sub>O in the oxide scale. Transport of H<sub>2</sub>O in the oxide scales can be due to the incorporation of hydrogen in the form of H<sup>+</sup> OH<sup>-</sup> or H<sub>2</sub>O [16, 22, 23]. It is assumed that protons might dissolve in the oxides and diffuse at grain boundaries. The low H<sup>+</sup> and OH<sup>-</sup> radii favour their diffusion through the oxide scale. Then, the protons presence in the scale can change the oxide defect chemistry and will be responsible of the change in the growth mechanism. According to some authors the grain size growth observed can be attributed to the oxygen vacancies annihilation in wet conditions according to equation 1. In our study, this can also be related to the more compact state of the zirconia present in the lamella formed in wet air [36].



In equation 1,  $s$  is an adsorption site on the surface of  $ZrO_2$ ,  $O_O$  an oxygen atom in the regular position in the oxide lattice,  $V_O^{**}$  a doubly ionized oxygen vacancy,  $OH_O^\bullet$  a hydroxide ion substitutional position.

## CONCLUSION

The present work have shown that during the Zircaloy-4 oxidation in dry and wet air at 700 °C the scale is composed of m- $ZrO_2$  and t- $ZrO_2$ . In wet air, the growth stress level is determined *in situ* at 700 °C on m- $ZrO_2$ . In dry air, the compressive growth stress varies periodically in the oxide between -1300 ±100 MPa and -600 ±100 MPa. In wet air, the compressive growth stress varies from -1000 ±100 MPa to -400 ±100 MPa after the 20 first hours of oxidation. Then, the stress level registered remains constant at -400 ±100 MPa as long as the high temperature is kept constant. In dry air stress oscillations can be explained by successive growth stress increase in the growing scale and stress relaxation by successive perpendicular cracks propagation. The higher zirconia grain size in the scale formed in wet air can explain that the growth stress relaxation process is different from the one observed in dry air.

## ACKNOWLEDGMENTS

The DENOPI project is a work funded by the French government as part of the "Investment for the Future" Program reference ANR-11-RSNR-0006.

## REFERENCES

1. S. Chevalier and J. Favregeon, *French Activity on High Temperature Corrosion in water Vapour*, Zürich, Trans Tech Publications, 2013 pp 75-129.
2. J. Godlewski, ASTM STP **1245**, 663 (1994).
3. S. Leistikow and G. Schanz, *Nuclear Engineering and Design* **103**, 65 (1987).
4. M. Steinbrück, *Oxidation of Metals* **70**, 317 (2008).
5. B. Cox, *Journal of Nuclear Materials* **148**, 332 (1987).
6. C. Duriez, T. Dupont, B. Schmet and F. Enoch, *Journal of Nuclear Materials* **380**, 30 (2008).
7. M. Parise, O. Sicardy and G. Cailletaud, *Journal of Nuclear Materials* **256**, 35 (1998).
8. J. P. Pemsler, *Electrochemical Technology* **4**, 128 (1966).
9. A. J. G. Maroto, R. Bordoni, M. Villegas, A. M. Olmedo, M. A. Blesa, A. Iglesias and P. Koenig, *Journal of Nuclear Materials* **229**, 79 (1996).
10. N. Pétigny-Putigny, «Comparaison de l'oxydation de deux alliages de zirconium par diffraction des rayons X in-situ et ex-situ : texture, phase, contrainte » PhD Thesis, Université de Bourgogne, France, 1998.
11. N. Pétigny-Putigny, P. Barberis, C. Lemaignan, C. Valot and M. Lallemand, *Journal of Nuclear Materials* **280**, 318 (2000).
12. A. Yilmazbayhan, A. T. Motta, R. J. Comstock, G. P. Sabol, B. Lai and Z. Cai, *Journal of Nuclear Materials* **324**, 6 (2004).
13. E. Polatidis, P. Frankel, J. Wei, M. Klaus, R.J. Comstock, A. Ambard, S. Lyon, R.A.Cottis and M. Preuss, *Journal of Nuclear Materials* **432**, 102 (2013).

14. J. Godlewski, J. Gros, M. Lambertin, J. Wadier and H. Weidinger, *ASTM Special Technical Publication* **1132**, 416 (1991).
15. I. Idarraga-Trujillo, « Etude des mécanismes de dégradation sous air à haute température des gaines de combustible nucléaire en alliage de zirconium » PhD Thesis, Université de Grenoble, France, 2011.
16. H. El Kadiri, Z. N. Utegulov, M. Khafizov, M. Asle Zaeem, M. Mamivand, L. Oppedal, K. Enakoutsa, M. Cherkaoui, R. H. Graham and A. Arockiasamy, *Acta Materialia* **61**, 3923 (2013).
17. I. Idarraga, M. Mermoux, C. Duriez, A. Crisci and J. P. Mardon, *Oxidation of Metals* **79**, 289 (2013).
18. H. Anada and K. Takeda, *ASTM Special Technical Publication* **1295**, 35 (1996).
19. A. Yilmazbayhan, E. Breval, A.T. Motta and R.J. Comstock, *Journal of Nuclear Materials* **349**, 265 (2006).
20. W. Qin, C. Nam, H. L. Li and J. A. Szpunar, *Acta Materialia* **55**, 1695 (2006).
21. M. Guerin, C. Duriez, J. L. Grosseau-Poussard and M. Mermoux, *Corrosion Science* **95**, 11 (2015).
22. S. Chevalier, J. Favergeon, French Activity on High Temperature Corrosion in water Vapour *French Activity on High Temperature Corrosion in water Vapour*, Zürich, Trans Tech Publications, 2013 pp 131-188.
23. Chun Liu, « Analyse des contraintes par diffraction des rayons X à haute température dans le système Ni-NiO » PhD Thesis, ENSAM Paris, 1991.
24. F. Bernard, E. Sciora and N. Gerard, *Journal de Physique IV* **C4**, 259 (1996).
25. C. Valot, « Technique de diffraction RX et dynamique spatio-temporelle de l'oxydation des métaux des groupes 4 et 5 – application au zirconium » PhD Thesis, Université de Bourgogne, 1995.
26. G. K. Williamson and W. H. Hall, *Acta Metallurgica* **1**, 22 (1953).
27. D. J. Spengler, A. T. Motta, R. Bajaj, J. R. Seidensticker and Z. Cai, *Journal of Nuclear Materials* **464**, 107 (2015).
28. C. Roy and G. David, *Journal of Nuclear Materials* **37**, 71 (1970).
29. C. Roy and B. Burgess, *Oxidation of Metals* **2**, 235 (1970).
30. B. Panicaud, J. L. Grosseau-Poussard, D. Retraint, M. Guerin and L. Li, *Corrosion Science* **68**, 263 (2012).
31. J. L. Béchade, P. Goudeau, M. Gailhanou and P. Yvon, *High Temperature Materials Processes* **2**, 59 (1998).
32. S. J. King, R. L. Kesterson, K.H. Yueh, R. J. Comstock, W. M. Herwig and S. D. Ferguson, *ASTM Special Technical Publication* **1423**, 471 (2002).
33. A. Methivier, « Etude expérimentale et théorique de l'évolution texturale et structurale des poudres de zircone pures et dopées » PhD Thesis, Ecole Nationale Supérieure des Mines de Saint Etienne, 1992.
34. R. Mevrel, *Materials Science and Technology* **3**, 531 (1987).
35. H. G. Jung and K. Y. Kim, *Oxidation of Metals* **46**, 147 (1996).
36. M. Tupin, M. Pijolat, F. Valdivieso, M. Soustelle, A. Frichet and P. Barberis, *Journal of Nuclear Materials* **317**, 130 (2003).